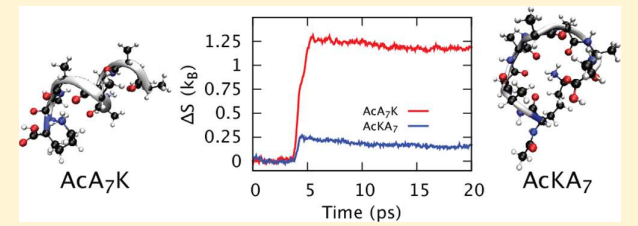
Cite This: J. Phys. Chem. B 2018, 122, 9549–9554

A Computational Comparison of Soft Landing of α -Helical vs Globular Peptides

Danielle Frederickson, Meghan McDonough, and George L. Barnes*

Department of Chemistry and Biochemistry, Siena College, 515 Loudon Road, Loudonville, New York 12211, United States

ABSTRACT: The effect of secondary structure on the soft landing process is investigated through direct dynamics simulations of AcA_7K and $AcKA_7$ colliding with a fluorinated, organic self-assembled monolayer (FSAM) surface. The α -helical (AcA_7K) and globular ($AcKA_7$) peptides each exhibited a similar probability of soft landing with normal incidence at all collision energies considered. Rapid conformational changes were quantified through the calculation of the time dependent, conformational entropy production that took



place during the collision events, which is consistent with the prior structural measurements made by Laskin and co-workers on these systems. AcA_7K produces more entropy during the collisions than $AcKA_7$.

1. INTRODUCTION

Tandem mass spectrometry is both a valuable analytical tool and a means of exploring the fundamentals of chemical dynamics in relatively high energy systems. ^{1–5} The application of mass spectrometry to systems of biological interest is an active field of study for both identification and characterization as well as a means to deposit biological molecules on a substrate via soft landing. ^{6–11} Direct dynamics simulations have been and continue to be a crucial tool that provides atomistic insight into the dynamics of tandem mass spectrometry systems. ¹²

Soft landing has a long experimental history.¹³ It has been exhibited to be a useful means to control the deposition of mass selected biological molecules on a substrate ⁹⁻¹¹ but has only recently been studied via direct dynamics simulations. Hase and co-workers, who pioneered peptide + organic self-assembled monolayer (SAM) direct dynamics simulations, have developed a new interaction potential between peptide ions and fluorinated SAM (FSAM) surfaces¹⁴ and went on to study the soft landing and energy transfer of dialanine.^{15,16}

In this work, we will make use of the same intermolecular potential energy surface and apply it to "large" systems that exhibit secondary structure. In particular, it has been shown by the Jarrold group that AcA_nK $(n \ge 7)$ adopts a stable α helix structure in the gas phase while AcKA, adopts a globular structure.¹⁷ Hence, a comparison of the dynamics of AcA_nK and AcKA, will largely provide insight into the role of secondary structure on the processes taking place. These are ideal systems for our study. Moreover, soft landing of these systems with n = 7 and 14 has been studied experimentally by Laskin and co-workers. While their study focused on the effect of the surface on the soft landing process, it will still serve as a useful comparison in the present work. In addition, their work suggests that conformational changes are occurring either during or after the soft landing event. This study provides insight into the time scale for that change.

While the n = 14 system would likely be computationally tractable, it would require a much larger computational expense without a clear gain in insight provided. Hence, we have selected AcA7K and AcKA7 as our model systems for this study. Below, we will investigate the conformational effect on soft landing as well as the time dependence of any conformational reorganization that takes place. In order to accomplish this latter goal, we make use of a method¹⁹ to calculate the conformational entropy for much larger systems and have adapted it to the ensemble of trajectories we calculate here. This technique provides a means to obtain a time dependent conformational entropy for each collision energy selected and shows that there is rapid entropy production that takes place during the trajectory. In addition, we will compare our findings to those of Hase in regard to the penetration of the peptide into the FSAM surface.

The outline for the remainder of the paper is as follows: in section 2, we provide an overview of our computational method, in section 3, we present and discuss our results, and last in section 4, we summarize the study.

2. COMPUTATIONAL DETAILS

We performed direct dynamics simulations of collisions between both structured and unstructured species with an FSAM surface using standard techniques^{20,21} and implemented the most recent peptide-FSAM intermolecular potential energy surface. Below, we will describe how we obtained our starting structure for the two peptides and give a brief overview of the simulation methodology.

2.1. Peptide Structures. Our goal is to investigate the effect of structure on soft landing. To this end, we are

Received: June 29, 2018 Revised: August 16, 2018 Published: August 22, 2018 comparing two acetylated peptides: AcA7K, and AcKA7. The similarity in size and chemical composition allows for a direct comparison, whereas the specific sequences result in either a stable, α helix structure (AcA₇K) or a random coil structure (AcKA7). In both cases, the excess proton is placed on the lysine side chain. The conformation for the structured peptide was constructed using Avogadro²² and optimized using the RM1²³ semiempirical method as implemented in Mopac2012.²⁴ The unstructured peptide was also initially drawn using Avogadro. This structure was used as input for a simulated annealing procedure performed using GROMACS²⁵ using the OPLS force field. One hundred heat-cool cycles were performed, ramping the temperature up to 1000 K over 100 ps and cooling down to 0 K over an additional 100 ps. The lowest energy conformation obtained from this procedure was then reoptimized at the RM1 level. We were not concerned with obtaining the global minimum structure, as we are seeking to investigate the differences between a highly structured species and an unstructured species. Figure 1 shows the two final structures obtained and used as input to the direct dynamics simulations.

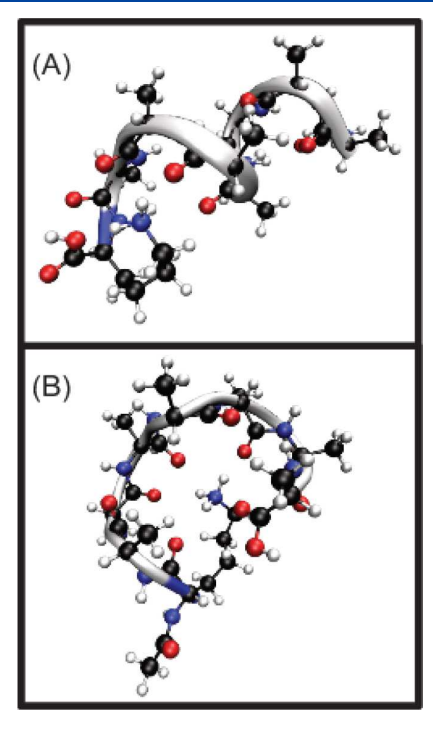


Figure 1. Minimum structures used for AcA_7K (A) and $AcKA_7$ (B). Both a "CPK" and "NewCartoon" representation, as implemented in VMD, are shown. The cartoon representation highlights the structural differences present between the two peptides. The color scheme for this figure and all others is as follows: C - black, H - white, N - blue, O - red, F - ochre.

2.2. Simulation Methodology. Our approach to performing direct dynamics simulations of collision systems relevant to mass spectrometry has recently been detailed in two review articles. Readers who are specifically interested in the application of this method to collisions between protonated peptides and self-assembled organic monolayers should also see several of the original works. Below, we will provide a brief overview of the method to place this work in context.

We begin by writing the potential energy as a sum of three components, namely,

$$V = V_{\text{peptide}} + V_{\text{SAM}} + V_{\text{peptide-SAM}} \tag{1}$$

where $V_{\rm SAM}$ is the well-established, intramolecular, molecular mechanical (MM) force field for FSAMs (see, for example, Yang et al. 28) and $V_{\rm peptide-SAM}$ is a recent MM force field developed by Hase and co-workers that is specifically designed for modeling soft landing. 14,16 The peptide potential, $V_{\rm peptide}$, is treated using a quantum mechanical (QM) method. We note that, while not strictly necessary for the present study, we are treating the peptide using a QM method such that future studies focused on peptide fragmentation of structured vs unstructured peptides can make direct comparisons to this work. Due to our prior success, $^{31-37}$ we will use the RM1 method.

The peptide is initially placed 40 Å above a 9×9 octanethiol FSAM surface with a random orientation. The surface is oriented such that the gold substrate is in the xy plane and the top of the surface is toward the positive zdirection. Initial positions and velocities were randomly selected for both the surface and the peptide using a velocity rescaling routine such that each was given an initial temperature of 300 K. Separate MD simulations were performed for the peptide and the surface with velocity rescaling occurring every 30 time steps. While this approach has previously been used for the surface, to our knowledge, this is the first time the approach has been applied to the peptide within this simulation framework. Typically, the initial conditions of the peptide are determined through use of the normal mode coordinates.³⁸ In this work, we chose to use velocity rescaling due to both the size of the peptide and the large number of small frequency vibrational modes. Twodimensional periodic boundary conditions were implemented to allow for soft landed peptides to diffuse on the surface. Lastly, a relative collision energy between 2.5 and 30 eV with a normal incidence angle was imparted to the peptide. Five hundred trajectories were calculated for each collision energy.

Hamilton's equations of motion were integrated using a sixth order sympletic integration scheme,³⁹ making use of a 1 fs step size with output written every 50 fs. Trajectories were stopped after 20 ps of simulation time. The vast majority of trajectories conserve energy to within 1% of the collision energy, while those that failed were recalculated with a 0.5 fs time step. All simulations were performed using an in-house simulation code coupled to Mopac2012.²⁴

3. RESULTS AND DISCUSSION

3.1. Probability of Soft Landing. The aim of this study is twofold: (1) to determine the importance of peptide structure on normal incidence soft landing efficiency and (2) to examine how the normal incidence soft landing process affects the conformation of the soft landed peptide. In order to accomplish these goals, it is necessary to develop a set of criteria to classify trajectories. We begin by presenting, in Figure 2, the z-coordinate for several representative trajectories that show the behavior of three classes of events that we have identified in the results. Note that, in this figure, zero is defined as the average position of the topmost carbon atom within the surface. The value was determined by performing a 300 K simulation of the surface alone and averaging the position.

The figure presents three classes, "direct bounce", "soft land", and "intermediate" which will be described and defined

The Journal of Physical Chemistry B

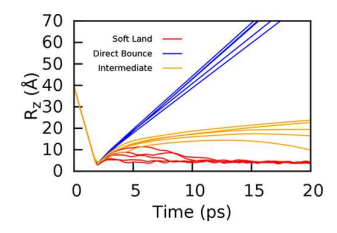


Figure 2. Representative examples of the z component of the center of mass of the peptide for direct bounce, soft land, and intermediate classes of trajectories. The ultimate fate of the intermediate trajectories would need longer time scale simulations to determine. Zero is defined to be the average z position of the topmost carbon atom within the surface.

below. There are clear differences in the behavior of these three classes with direct bounce exhibiting what appears to be largely repulsive interactions that result in a simple bounce off the surface, while the soft landed trajectories either bounce off and are pulled back or stay relatively close the entire time. It is striking that some soft landed trajectories take several picoseconds to return to the surface and that the center of mass moves more than 10 Å away. Intermediate trajectories are trajectories that will either eventually be pulled back to the surface or ultimately escape from the surface but have experienced more than one inner turning point. As our simulations only go out to 20 ps and the population in this class is relatively small, we did not attempt to differentiate these two possible outcomes.

Figure 2 illustrates an obstacle to the analysis: the peptide's center of mass can move a significant distance away from the surface and still experience enough of an attractive interaction to ultimately become soft landed. Hence, using simple distance cutoffs to classify our trajectories was problematic. To overcome this issue, we have developed criteria that do not make use of distance directly but rather the number of inner turning points that occur in a trajectory and the magnitude of the MM interaction between the peptide and the surface, namely, $V_{\rm peptide-SAM}$.

In order to be classified as a direct bounce event, the peptide must be moving in the positive z direction at the end of the trajectory and have a single inner turning point. In trajectories that were classified as a soft landing event, the peptide must have had more than one inner turning point as well as a final $V_{\text{peptide-SAM}} < -3 \text{ kcal/mol}$. Using the MM interaction energy proved to be a simple and effective means of determining if the peptide was either close to the surface or experiencing a large favorable interaction. The cutoff value was arbitrarily determined, but the results are not sensitive to the value as long as it is chosen to be a small, negative value. The average $V_{\rm peptide-SAM}$ for soft landed trajectories at 20 eV is -36.6 kcal/ mol. The last class, intermediate, also have more than one inner turning point but have a final $V_{\text{peptide-SAM}} \ge -3 \text{ kcal/mol}$, which means that the peptide is either far away from the surface or does not exhibit strong attractive interactions. The average $V_{\text{peptide-SAM}}$ for intermediate trajectories at 20 eV is -0.54 kcal/mol. Given that there is still an attractive interaction present at the end of the trajectory, it is unclear if the peptide will ultimately escape or if it will be pulled back to the surface. The vast majority of trajectories fall into one of the first two classes, as seen in Figure 3, which shows the fraction of trajectories within each class as a function of collision energy for the AcA₇K peptide. The fraction of "soft

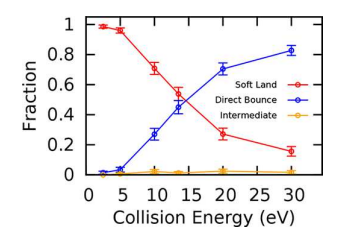


Figure 3. Probability of direct bounce, soft land, and intermediate trajectories for AcA₇K as a function of collision energy. Within the error bars of the simulation, AcA₇K and AcKA₇ have identical fractions within each class.

land" strongly decreases with collision energy, while the fraction of "direct bounce" strongly increases with collision energy. We note that the fractions for AcA_7K and $AcKA_7$ are nearly identical and within the error bars for each other, and hence, we conclude that the conformation of the peptide has little effect on the probability of successful soft landing.

A comparison of the present results with those for the dialaine work 16 make it possible to gain some insight into the effect of size on soft landing efficiency. Generally speaking, the two works show qualitatively similar trends. Hence, we will make a comparison for the 13.5 eV collision energy, which has a roughly equal population between soft land and direct bounce. Table 1 from ref 16 reports a soft landing fraction of 0.65 \pm 0.02, whereas this work finds a fraction of 0.54 \pm 0.04, which suggests that the soft landing efficiency has slightly decreased due to either the size or conformation of the larger peptide.

3.2. Conformational Changes That Result from **Collision.** We now turn our attention to examining the conformational changes that may take place during the collision event. There is a great variability in conformational changes, which makes it difficult to both generalize and succinctly describe. Various approaches were taken, including tracking distance variations, calculating the radius of gyration as well as the asymmetry parameter—which describes oblate vs prolate shapes using the rotational constants. However, none of these approaches produced a straightforward description of the changes taking place. One generalization that can be made is that, on average, the radius of gyration increases following the collision for both direct bounce and soft landed trajectories as well as for both α -helical and globular peptides. For AcA₇K, the helical nature is also quickly lost but results in either a straight-chain-like or globular configuration.

Due to the large variability in the type of conformational changes observed, we sought a method to quantify the relative magnitude of the change. Our approach to quantifying the magnitude of change in secondary structure makes use of the Ramachandran angles of the peptide backbone. We calculate a time dependence of each angle for each trajectory and use them to develop a time dependent probability distribution, $P(\phi, \psi, t)$, for each collision energy. Given the small size of our system, a single trajectory will not provide a good means of obtaining the probability distribution. However, by combining the results from all trajectories for each collision energy, we obtain a meaningful probability distribution for the given collision energy. In this work, we only make use of the soft landed trajectories to calculate the probability distribution.

With the probability distribution on hand, the conformational statistical entropy is calculated as $S(t) = -k_{\rm B} \sum_i P_i(t) \ln(P_i(t))$, where P_i is the probability of being found in a

particular ϕ , ψ bin. It has been shown that ΔS is independent of bin size. ¹⁹ We divide ϕ , ψ space into 225 bins, and the 300 K entropy for each peptide (i.e., the initial state of each trajectory) is used as a reference to create a time dependent ΔS function for each collision energy. This choice of reference focuses on the entropy production that takes place during the trajectory and highlights the relative change in entropy for each peptide. We note that AcA7K has a smaller entropy than AcKA₇ at 300 K. Figure 4 compares the entropy production of

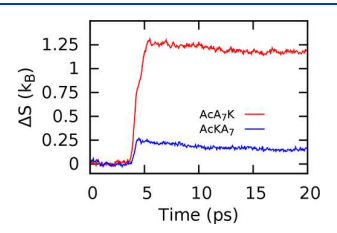


Figure 4. Relative entropy production of each peptide at 2.5 eV. The structured peptide has a larger entropy production during the course of the trajectory.

soft landed peptides for AcA7K and AcKA7 at 2.5 eV. At this collision energy, nearly all peptides are soft landed. Prior to the collision, both systems exhibit small fluctuations about zero, which is consistent with normal thermal variations for a small population at 300 K. Once the peptide has reached the surface, we observe a dramatic increase in entropy for both systems. Although both systems exhibit very fast increases in entropy, AcA7K has a much larger increase than AcKA7. Once the increase has peaked, a very slight decrease in entropy is seen, followed by relatively stable thermal fluctuations for the remainder of the time frame. The rate of entropy change, and hence conformational change, is striking.

The magnitude of the entropy production can also be examined as a function of collision energy, as shown in Figure 5. Again, we focus on the soft land class and show the time

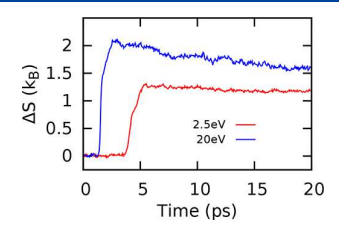


Figure 5. Relative entropy production of AcA7K at 2.5 and 20 eV. The same qualitative shape of the entropy production curve is seen, though the magnitude of the change is much greater for the higher collision energy.

dependent entropy production for 2.5 and 20 eV collisions. Both are qualitatively similar, though the magnitude of the change is greater for the larger collision energy. We selected this collision energy because the soft land population is still large enough to be meaningful. This plot also shows that the decrease in entropy following the peak is more pronounced with larger collision energy and suggests that additional reorganization may take place on a time scale longer than our simulation. The reorganization that is seen can result in a significant loss of entropy, as seen from a peak of $\sim 2 k_B$ and an ending value of $\sim 1.5 k_{\rm R}$.

We noted above that, by making the reference entropy different for each peptide, we are focusing on the entropy generated by the collision event. AcA7K generates more entropy than AcKA7, which is in part due to having a more ordered starting structure that exhibits strong intramolecular interactions. It is also possible to examine the "absolute" entropy production by defining the reference state to be AcA7K at 300 K. The absolute entropy production for each peptide and collision energy is shown in Table 1.

Table 1. Absolute Entropy, in Units of k_B , for AcA₇K and AcKA₇ Using the 300 K AcA₇K Structure as the Reference^a

	AcA ₇ K		AcKA ₇	
collision energy (eV)	$k_{ m B}^{ m i}$	$k_{ m B}^{ m f}$	$k_{ m B}^{ m i}$	$k_{ m B}^{ m f}$
2.5	0.00	1.19	0.79	0.96
5	0.04	1.21	0.78	0.95
10	-0.03	1.48	0.77	0.94
13.5	0.03	1.54	0.76	0.96
20	0.00	1.61	0.78	0.95

^aBoth the initial (k_b^i) and final (k_b^f) entropy values are shown. Although two decimal places are shown, the values are only accurate to one.

The absolute entropy analysis shows that the entropy production for AcKA7 is roughly constant with collision energy, while that for AcA7K increases. Again, this is due to the nature of the starting structures. AcA7K had more of an ordered structure to lose and will also take a longer time to reorganize following the rapid loss of that structure. This analysis also shows that, while the entropy gained by AcA₇K is much larger than that gained by AcKA7, they end up in a somewhat similar disordered state at the end of the trajectory.

3.3. Penetration of the Peptide into the Surface. The previous simulations involving soft landing of dialanine on an FSAM surface provided a detailed analysis of the penetration depth of their peptide. Here we provide a comparison to that work. A comparison of Figure 2 of this work and Figure 1 of Pratihar and co-workers 16 immediately shows qualitative differences between the smaller dialanine system and those studied here. For the smaller system, during the collision, the peptide penetrates below the capping -CF₃ groups for all classes of trajectory by as much as 3-5 Å. However, that is not seen for AcA₇K or AcKA₇. In fact, the center of mass for these larger systems stays a similar amount above the capping -CF₃ groups. Given that we are using the same intermolecular potential energy surface and the same surface structure and have peptides that have largely the same chemical composition when discounting the lysine group, this effect is entirely due to the sizes of the peptides. One possible reason for the differences seen is that the work of Pratihar and co-workers did extend to significantly higher collision energies than those in this study; however, the above comparison is at the same collision energy. Our penetration analysis does show that there is greater "penetration" at higher collision energy, but even at our largest collision energy, the center of mass of the peptide is still above the top of the surface. In order to further investigate penetration, we also tracked the minimum height of heavy atoms within the peptide, which would represent the deepest depth that the peptide penetrates into the surface. Again, we find that there is little penetration into the surface with typical trajectories moving down to the height of the 300 K average height of the terminal carbon, or slightly below, on impact before moving back up from this level. This is qualitatively similar to the behavior seen by Hase and co-workers ¹⁶ for dialanine. In that work, at a collision energy of 30 eV, over 75% showed no penetration. It is not surprising that this would be further decreased by a larger peptide. When examining the average distance of closest approach between AcA₇K and AcKA₇, the two peptides have nearly identical results. In contrast, soft landed trajectories have a smaller average distance of closest approach; for example, at a collision energy of 13.5 eV, where the two peptides have close to the same population in each class, the center of mass for soft landed trajectories gets \sim 0.2 Å closer to the top of the surface.

In the dialanine work, penetration into the surface was used to describe the mechanism for soft landing. Since we do not see the same type of penetration as that work, our mechanisms for soft landing all primarily involve physisorption to the surface. We also observe an interesting class of soft landed trajectories that we call "tethering" in which either a single or a small number of atoms experience a strong attractive interaction with the surface while the remainder of the peptide is relatively far away from the surface. An example of this type of event is shown in Figure 6. This class of event likely was not seen, or at least was not as dramatic, for the smaller system.

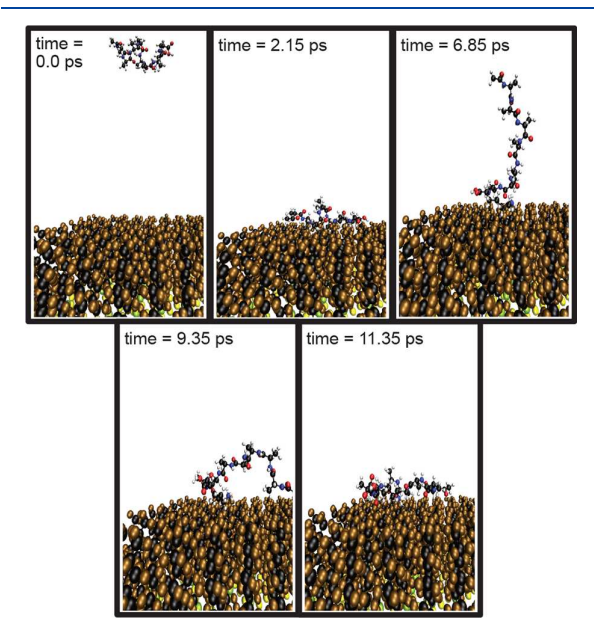


Figure 6. Snapshots taken from a 13.5 eV trajectory that illustrates the "tethering" mechanism for soft landing. By 2.15 ps, the peptide has reached the surface and experienced enough repulsion for the majority to begin to move away from the surface. At 6.85 ps, the "tethering" occurs, which happens to take place via the lysine side chain for this trajectory. At 9.35 ps, the N-terminus begins interacting with the surface, while the center of the chain is fairly remote, but by 11.35 ps, the peptide is largely flat against the surface. The yellow and light green atoms visible are gold and sulfur, respectively.

4. SUMMARY

Our simulations have shown that both α -helical and globular peptides have nearly identical soft landing fractions at all collision energies considered within our study. The classification of trajectories was accomplished on the basis of the number of inner turning points and the magnitude of the MM

interaction between the peptide and the surface. Not surprisingly, soft landing is favored at low collision energies, while direct bounce is preferred at large collision energies.

We have developed a means of tracking the time dependent conformational entropy and have used these time curves to examine the conformational changes that take place during the collision. A fast and dramatic increase in entropy is observed for both peptides with AcA_7K experiencing a larger magnitude change, though both peptides have reasonably similar absolute entropies at the end of the trajectory for low collision energies. We expect that, if the simulation time was increased significantly, the absolute entropy of these two peptides would be similar. This suggests that the final conformation of the two would also be similar, which is in agreement with the experimental results of Laskin and co-workers. 18

A comparison was made to the previous work of Hase and co-workers, specifically in regard to the penetration of the peptide into the surface. Due to the size difference between the dialanine studied previously and our AcA₇K and AcKA₇, qualitative differences were observed. Hence, the primary mechanism for soft landing for this system is through physisorption to the surface. We also described a "tethering" mechanism in which an initially small number of atoms are strongly attracted to the surface prior to the entire peptide becoming physisorbed.

In future work, it would be of interest to explore the slow reorganization process that is seen in our plots of the entropy for large collision energies. In addition, although we saw little effect on the soft landing efficiency as a function of secondary structure, the surface induced dissociation process may be more sensitive to structure.

AUTHOR INFORMATION

Corresponding Author

*E-mail: gbarnes@siena.edu.

ORCID ®

George L. Barnes: 0000-0001-9211-2736

Notes

The authors declare no competing financial interest.

ACKNOWLEDGMENTS

G.L.B. gratefully acknowledges support from the National Science Foundation under Grant No. 1763652 as well as insightful conversations with Dr. Julia Laskin. Network infrastructure was enhanced by NSF grant number CC*DNI-1541001. D.F. and M.M. acknowledge support through the Siena Summer Scholars Program.

REFERENCES

- (1) Laskin, J.; Denisov, E.; Futrell, J. H. Comparative Study of Collision-Induced and Surface-Induced Dissociation. 2. Fragmentation of Small Alanine-Containing Peptides in FT-ICR MS. *J. Phys. Chem. B* **2001**, *105*, 1895–1900.
- (2) Laskin, J.; Bailey, T. H.; Futrell, J. H. Shattering of Peptide Ions on Self-Assembled Monolayer Surfaces. *J. Am. Chem. Soc.* **2003**, *125*, 1625–1632.
- (3) Laskin, J.; Futrell, J. H. Surface-Induced Dissociation of Peptide Ions: Kinetics and Dynamics. *J. Am. Soc. Mass Spectrom.* **2003**, *14*, 1340–1347.
- (4) Laskin, J.; Futrell, J. H. Collisional Activation of Peptide Ions in FT-ICR Mass Spectrometry. *Mass Spectrom. Rev.* **2003**, 22, 158–181.
- (5) Laskin, J.; Futrell, J. H. Energy Transfer in Collisions of Peptide Ions with Surfaces. *J. Chem. Phys.* **2003**, *119*, 3413–3420.

- (6) Ouyang, Z.; Takáts, Z.; Blake, T. A.; Gologan, B.; Guymon, A. J.; Wiseman, J. M.; Oliver, J. C.; Davisson, V. J.; Cooks, R. G. Preparing Protein Microarrays by Soft-Landing of Mass-Selected Ions. *Science* **2003**, *301*, 1351–1354.
- (7) Gologan, B.; Takáts, Z.; Alvarez, J.; Wiseman, J. M.; Talaty, N.; Ouyang, Z.; Cooks, R. G. Ion Soft-Landing into Liquids: Protein Identification, Separation, and Purification with Retention of Biological Activity. *J. Am. Soc. Mass Spectrom.* **2004**, *15*, 1874–1884.
- (8) Volný, M.; Elam, W. T.; Ratner, B. D.; Turecek, F. Preparative Soft and Reactive Landing of Gas-Phase Ions on Plasma-Treated Metal Surfaces. *Anal. Chem.* **2005**, *77*, 4846–4853.
- (9) Wang, P.; Hadjar, O.; Laskin, J. Covalent Immobilization of Peptides on Self-Assembled Monolayer Surfaces Using Soft-Landing of Mass-Selected Ions. *J. Am. Chem. Soc.* **2007**, *129*, 8682–8683.
- (10) Wang, P.; Laskin, J. Helical Peptide Arrays on Self-Assembled Monolayer Surfaces Through Soft and Reactive Landing of Mass-Selected Ions. *Angew. Chem., Int. Ed.* **2008**, *47*, 6678–6680.
- (11) Laskin, J.; Wang, P.; Hadjar, O. Soft-Landing of Peptide Ions Onto Self-Assembled Monolayer Surfaces: An Overview. *Phys. Chem. Chem. Phys.* **2008**, *10*, 1079–1090.
- (12) Pratihar, S.; Barnes, G. L.; Hase, W. L.; Pratihara, S.; Barnes, G. L.; Hase, W. L. Chemical Dynamics Simulations of Energy Transfer, Surface-Induced Dissociation, Soft-Landing, and Reactive- Landing in Collisions of Protonated Peptide Ions with Organic Surfaces. *Chem. Soc. Rev.* **2016**, *45*, 3595–3608.
- (13) Miller, S. A.; Lou, H.; Pachuta, S. J.; Cooks, R. G. Soft-Landing of Polyatomic Ions at Fluorinated Self-Assembled Monolayer Surfaces. *Science* **1997**, *275*, 1447–1450.
- (14) Pratihar, S.; Kohale, S. C.; Vázquez, S. A.; Hase, W. L.; Va, S. A.; Hase, W. L. Intermolecular Potential for Binding of Protonated Peptide Ions with Perfluorinated Hydrocarbon Surfaces. *J. Phys. Chem. B* **2014**, *118*, 5577–5588.
- (15) Pratihar, S.; Kohale, S. C.; Bhakta, D. G.; Laskin, J.; Hase, W. L. Dynamics of Energy Transfer and Soft-Landing in Collisions of Protonated Dialanine with Perfluorinated Self-Assembled Monolayer Surfaces. *Phys. Chem. Chem. Phys.* **2014**, *16*, 23769–78.
- (16) Pratihar, S.; Kim, N.; Kohale, S. C.; Hase, W. L. Mechanistic Details of Energy Transfer and Soft Landing in ala₂-H⁺ Collisions with a F-SAM Surface. *Phys. Chem. Chem. Phys.* **2015**, *17*, 24576–24586.
- (17) Hudgins, R. R.; Jarrold, M. F. Helix Formation in Unsolvated Alanine-Based Peptides: Helical Monomers and Helical Dimers. *J. Am. Chem. Soc.* **1999**, *121*, 3494–3501.
- (18) Hu, Q.; Wang, P.; Laskin, J. Effect of the Surface on the Secondary Structure of Soft Landed Peptide Ions. *Phys. Chem. Chem. Phys.* **2010**, *12*, 12802–12810.
- (19) Baxa, M. C.; Haddadian, E. J.; Jumper, J. M.; Freed, K. F.; Sosnick, T. R. Loss of Conformational Entropy in Protein Folding Calculated Using Realistic Ensembles and its Implications for NMR-Based Calculations. *Proc. Natl. Acad. Sci. U. S. A.* **2014**, *111*, 15396–15401.
- (20) Bolton, K.; Hase, W. L.; Peslherbe, G. H. In *Mod. Methods Multidimens. Dyn. Comput. Chem.*; Thompson, D. L., Ed.; World Scientific: Singapore, 1998; pp 143–189.
- (21) Sun, L.; Hase, W. L. Born-Oppenheimer Direct Dynamics Classical Trajectory Simulations. *Rev. Comput. Chem.* **2003**, *19*, 79–146.
- (22) Hanwell, M. D.; Curtis, D. E.; Lonie, D. C.; Vandermeersch, T.; Zurek, E.; Hutchison, G. R. Avogadro: An Advanced Semantic Chemical Editor, Visualization, and Analysis Platform. *J. Cheminf.* **2012**, *4*, 17.
- (23) Rocha, G. B.; Freire, R. O.; Simas, A. M.; Stewart, J. J. P. RM1: A Reparameterization of AM1 for H, C, N, O, P, S, F, Cl, Br, and I. J. Comput. Chem. **2006**, *27*, 1101–1111.
- (24) Stewart, J. P. Mopac2012; 2012; http://openmopac.net (accessed Aug 7, 2018).
- (25) Hess, B.; Kutzner, C.; van der Spoel, D.; Lindahl, E. GROMACS 4: Algorithms for Highly Efficient, Load-Balanced, and Scalable Molecular Simulation. J. Chem. Theory Comput. 2008, 4, 435–447.

- (26) Pratihar, S.; Barnes, G. L.; Laskin, J.; Hase, W. L. Dynamics of Protonated Peptide Ion Collisions with Organic Surfaces. Consonance of Simulation and Experiment. *J. Phys. Chem. Lett.* **2016**, *7*, 3142–3150
- (27) Barnes, G. L.; Hase, W. L. Energy Transfer, Unfolding, and Fragmentation Dynamics in Collisions of N-Protonated Cctaglycine with an H-SAM Surface. *J. Am. Chem. Soc.* **2009**, *131*, 17185–17193.
- (28) Yang, L.; Mazyar, O. A.; Lourderaj, U.; Wang, J.; Rodgers, M. T.; Martinez-Núñez, E.; Addepalli, S. V.; Hase, W. L. Chemical Dynamics Simulations of Energy Transfer in Collisions of Protonated Peptide Ions with a Perfluorinated Alkylthiol Self-Assembled Monolayer Surface. J. Phys. Chem. C 2008, 112, 9377–9386.
- (29) Meroueh, O.; Hase, W. L. Effect of Surface Stiffness on the Efficiency of Surface-Induced Dissociation. *Phys. Chem. Chem. Phys.* **2001**, 3, 2306–2314.
- (30) Meroueh, O.; Hase, W. L. Dynamics of Energy Transfer in Peptide-Surface Collisions. J. Am. Chem. Soc. 2002, 124, 1524–1531.
- (31) Barnes, G. L.; Podczerwinski, A. Simulating the Effect of Charge State on Reactive Landing of a Cyclic Tetrapeptide on Chemically Modified Alkylthiolate Self-Assembled Monolayer Surfaces. J. Phys. Chem. C 2017, 121, 14628–14635.
- (32) Homayoon, Z.; Pratihar, S.; Dratz, E.; Snider, R.; Spezia, R.; Barnes, G. L.; Macaluso, V.; Martin Somer, A.; Hase, W. L. Model Simulations of the Thermal Dissociation of the TIK(H⁺)₂ Tripeptide: Mechanisms and Kinetic Parameters. *J. Phys. Chem. A* **2016**, *120*, 8211–8227.
- (33) Shaikh, K.; Blackwood, J.; Barnes, G. L. The Effect of Protonation Site and Conformation on Surface-Induced Dissociation in a Small, Lysine Containing Peptide. *Chem. Phys. Lett.* **2015**, *6*37, 83–87.
- (34) Gregg, Z.; Ijaz, W.; Jannetti, S.; Barnes, G. L. The Role of Proton Transfer in Surface-Induced Dissociation. *J. Phys. Chem. C* **2014**, *118*, 22149–22155.
- (35) Geragotelis, A.; Barnes, G. L. Surface Deposition Resulting from Collisions Between Diglycine and Chemically Modified Alkylthiolate Self-Assembled Monolayer Surfaces. *J. Phys. Chem. C* **2013**, *117*, 13087–13093.
- (36) Ijaz, W.; Gregg, Z.; Barnes, G. L. Complex Formation during SID and Its Effect on Proton Mobility. *J. Phys. Chem. Lett.* **2013**, *4*, 3935–3939.
- (37) Barnes, G. L.; Young, K.; Yang, L.; Hase, W. L. Fragmentation and Reactivity in Collisions of Protonated Diglycine with Chemically Modified Perfluorinated Alkylthiolate-Self-Assembled Monolayer Surfaces. J. Chem. Phys. 2011, 134, 094106.
- (38) Peslherbe, G. H.; Wang, H.; Hase, W. L. Monte Carlo Sampling for Classical Trajectory Simulations. *Adv. Chem. Phys.* **2007**, *105*, 171–201.
- (39) Schlier, C.; Seiter, A. High-Order Symplectic Integration: An Assessment. *Comput. Phys. Commun.* **2000**, *130*, 176–189.
- (40) Ramachandran, G. N.; Ramakrishnan, C.; Sasisekharan, V. Stereochemistry of Polypeptide Chain Configurations. *J. Mol. Biol.* **1963**, *7*, 95–99.